International Journal of Pharmaceutics 672 (2025) 125303

Contents lists available at ScienceDirect

International Journal of Pharmaceutics

journal homepage: www.elsevier.com/locate/ijpharm

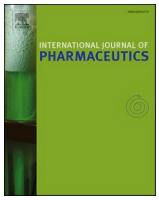

Using density changes to monitor blending with magnesium stearate by terahertz time-domain spectroscopy

Moritz Anuschek [a,b,*], Thea Nilsson [b], Anne Linnet Skelbæk-Lorenzen [b], Thomas Kvistgaard Vilhelmsen [b], J.Axel Zeitler [c], Jukka Rantanen [a]

[a] Department of Pharmacy University of Copenhagen Copenhagen Denmark
[b] Novo Nordisk A/S ET Oral Product Development Måløv Denmark
[c] Department of Chemical Engineering and Biotechnology University of Cambridge Cambridge UK

A B S T R A C T

Magnesium stearate (MgSt) is among the most common excipients and the most common lubricant in solid oral products. It is primarily added to tablet formulations to ease ejection during tablet compression. While commonly present in low concentrations, the addition of MgSt substantially affects the final tablet properties. Its impact is further not only concentration dependent but also varies with exposure of the formulation to shear, which worst-case results in over-lubrication. The presented study investigated the applicability of terahertz time-domain spectroscopy (THz-TDS) to monitor the shear-induced blend densification of microcrystalline cellulose blended with MgSt over a range of concentrations (0.3, 0.7, and 1.0 %). The effect of shear was investigated by variation of blending times (5 – 20 min) in a diffusion blender. THz-TDS measurements of the powder blends were acquired in transmission by measuring directly through the mixing container. The refractive index at terahertz frequencies was found to be sufficiently sensitive to resolve the densification of the blend with increased blending times. Thus, THz-TDS blend density measurements can be used as a surrogate parameter to evaluate the total shear exposure of a blend. Considerations regarding implementation are discussed. In the context the approach was integrated with the well-described THz-TDS-based tablet porosity analysis into a unified model to monitor and predict the tensile strength. Including the THz-TDS measurement on the blend allowed for a more accurate description of the tensile strength, reducing the root mean squared error by over 40 % (0.33 MPa). The possibility of monitoring the density changes of a blend non-invasively makes THz-TDS a promising process analytical technology approach for controlling the total shear impact on lubricated blends and tablet quality.

1. Introduction

The final steps of the tablet compression cycle are the ejection of the tablet from the die and the subsequent take-off from the lower punch. During these steps, the movement of the tablet relative to the tooling surfaces creates friction, which may damage the tablet and the tooling. During tablet manufacturing, high friction, often manifesting itself in high ejection forces, can be reduced by the addition of lubricants (Wang et al. 2010). Whilst the concept of external lubrication, where a lubricant is mechanically applied directly to the tooling before each compaction cycle, has been demonstrated in principle for different lubricants (De Backere et al. 2020; De Backere et al. 2023a), the realisation of external lubrication on a commercial scale remains challenging. Therefore, internal lubrication, the traditional approach where the lubricant is mixed into the formulation, prevails in the commercial manufacture of tablets (De Backere et al. 2020). Besides high ejection forces, the adhesion of formulation particles to the punches and die surfaces (sticking and picking) is a common challenge during tablet ejection and take-off. Addition of lubricants to the formulation may prevent this due to the anti-adhering properties of most lubricants (Shah et al. 1986).

Magnesium stearate (MgSt) is the most commonly used excipient to avoid complications during tablet ejection and take-off. Low concentrations (< 1 %) of MgSt typically suffice to improve the compression process (De Backere et al. 2023b; Li and Wu 2014; Sun 2015; Wang et al. 2010). Due to its friction-reducing properties (Wang et al. 2010) MgSt is generally classified as a lubricant (Raymond et al., 2009), but it also exhibits excellent anti-adherent (Shah et al. 1986) and glidant properties (Podczeck and Mia 1996). MgSt is a solid, organo-metallic salt of magnesium and a blend of fatty acids containing a high percentage of stearic and palmitic acid (European Pharmacopoeia, 2024). As with other solid lubricants, its effects on the formulation arise from boundary lubrication (Wang et al. 2010). Already at very low shear forces, the MgSt crystal lattice is cleaved, resulting in detached, plate-like particles (flakes) (Wada and Matsubara 1994; Marwaha and Rubinstein 1987). This detachment occurs during blending and other shear-inducing process steps, with the resulting MgSt-flakes subsequently adhering to other

* Corresponding author.
E-mail addresses: moritz-anuschek@gmx.de, NTAH@novonordisk.com (M. Anuschek).

https://doi.org/10.1016/j.ijpharm.2025.125303
Received 24 November 2024; Received in revised form 18 January 2025; Accepted 29 January 2025
Available online 31 January 2025

Nomenclature

Abbreviations

BF	Breaking force
c	Speed of light
CMA	Critical material attribute
CQA	Critical quality attribute
CPP	Critical process parameter
D	Diameter
EMA	European Medicines Agency
FDA	U.S. Food and Drug Administration
$f_{nominal}$	Nominal porosity
H	Height
HDPE	High-density polyethylene
ICH	International Council for Harmonisation of Technical Requirements for Pharmaceuticals for Human Use
IQA	Critical quality attribute of intermediate
l	Sample length or thickness
m	Mass
MBSD	Moving block standard deviation
MCC	Microcrystalline cellulose
MgSt	Magnesium stearate
N_B	Block size
n_{Blend}	Refractive index of the blend
n_{Tablet}	Refractive index of the tablet
NIR	Near infrared
QbD	Quality by Design
QbT	Quality by Testing
R^2	Coefficient of determination
RMSE	Root mean squared error
$RMSE_{adj}$	Root mean squared error adjusted for the number of fitting parameters
RTR	Real-time release
PAT	Process analytical technology
Ph. Eur.	European Pharmacopoeia
THz-TDS	Terahertz time-domain spectroscopy
USP	United states pharmacopeia
$\Delta\Phi$	Phase difference
ν	Frequency
Φ_{Blend}	Phase of blend inside HDPE container
Φ_{HDPE}	Phase of empty HDPE container
$\Phi_{R,Blend}$	Phase of empty chamber prior to blend measurement (reference)
$\Phi_{R,HDPE}$	Phase of empty chamber prior to HDPE container measurement (reference)
$\Phi_{R,Tablet}$	Phase of empty chamber prior to the tablet measurement (reference)
Φ_{Tablet}	Phase of the tablet
ρ_{pyc}	Pycnometric density
ρ_{tapped}	Tapped bulk density
$\rho_{untapped}$	Untapped bulk density
σ	Tensile strength
σ_{pred}	Predicted tensile strength

particles of the formulation and the tooling surface, i.e. boundary lubrication and often referred to as film formation. This layer reduces adhesive interactions as well as the particle–particle and particle-tooling contact area. Consequently, friction and powder adherence are reduced (Wang et al. 2010). While the structure of MgSt trihydrate has been solved (Herzberg et al. 2023), there is no solved crystal structure for the typical commercial grade of MgSt (hydrates with a varying molar ratio of water in the blend of fatty acids). Therefore, the exact nature of the lattice cleavage, flake formation, and adhesion to other particles, remains unresolved.

The adherence of MgSt to the other particles of the tablet formulation may have deteriorating effects on the drug product and MgSt has a substantial influence on tablet properties even at low concentrations. It has been found to decrease tablet mechanical strength and to slow down tablet disintegration and dissolution due to hydrophobicity of the fatty acid entities (Dansereau and Peck 1987; Puckhaber et al. 2022; Puckhaber et al. 2023; Abe and Otsuka 2012; Strickland et al., 1956; Uzunović and Vranić 2007). It is well known that the effects of MgSt on powder manufacturability and tablet properties highly depend on the total amount of shear the system is exposed to before tablet compression. Upon shear exposure flakes continuously detach from larger MgSt particles and adsorb on the other particles causing a higher surface coverage (Hafeez Hussain et al. 1988). Increased shear has been found to result in decreased ejection forces, decreased mechanical strength, and increased disintegration and dissolution times (Kushner IV and Moore, 2010; Mehrotra et al. 2007; Dansereau and Peck 1987; Paul and Sun 2018; Shah and Mlodozeniec 1977; Puckhaber et al. 2023). Overlubrication is a term used when the applied concentration or shear is too high and results in unacceptable tablet properties. In addition, an increased shear exposure or higher MgSt concentration has been found to affect blend flowability (Fahiq et al. 2007; Podczeck and Mia 1996). Finally, a densification of the blend due to increased shear exposure or higher MgSt concentration was described in various studies (Shah and Mlodozeniec 1977; Dansereau and Peck 1987; Mehrotra et al. 2007; Kushner IV, 2012).

The pharmaceutical industry is currently undergoing two transitions – from Quality by Testing (QbT) to Quality by Design (QbD) (Yu, 2008) and from batch to continuous manufacturing (Fonteyne et al. 2015; Plumb 2005; Lee et al. 2015) – both developments heavily encouraged by regulatory authorities (FDA 2004a) and the ICH (ICH Q8 2009; ICH Q8, Q9, Q10 Questions and Answers 2011; ICH Q13 2023; ICH Q14 2024). Implementing a continuous process is considered beneficial from an industrial and regulatory perspective by reducing monetary and time investment, and by increasing agility, flexibility, quality, understanding, and robustness of pharmaceutical manufacturing (Lee et al. 2015; Fonteyne et al. 2015). Continuous manufacturing is inherently linked to the transition from QbT to QbD as it necessitates understanding of critical process parameters and raw material or intermediate product quality attributes to ensure high product quality (Lee et al. 2015; Su et al. 2019; Yu 2008). The pharmaceutical industry and regulatory agencies acknowledge that these transitions require novel process analytical technology (PAT) tools that allow a detailed analysis of raw materials, intermediates, the process, and the product (Hinz 2006; FDA 2004b). Implementing PAT tools is believed to facilitate process and product understanding, ultimately, allowing the establishment of real-time monitoring of critical quality and material attributes, as well as critical process parameters. Incorporating PAT strategies and continuous manufacturing can further enable real-time release (RTR) testing. In RTR testing, PAT-based monitoring strategies ensure that the process continuously produces a drug product within quality specifications (ICH Q8 2009; Markl et al. 2020). This requires the development of "fit--for-purpose" PAT procedures, based on prior knowledge of the product, process, and analytical procedure as outlined in ICH Q14.

During powder blending, the API content and blend uniformity are considered relevant quality attributes to monitor due to their direct link to the content and content uniformity of the drug product (Kim et al. 2021). Although the excipient concentration and their blend homogeneity can significantly influence the finished product, they are commonly not monitored through in-process controls. Since the extent of powder lubrication can directly influence the quality of produced

tablets it would be beneficial to monitor lubrication during the manufacturing process independent of the production setup being batch-wise or continuous. In common process conrol strategies, variations in lubricant concentration or shear exposure may only be found by testing the finished tablet product. Incorporating a PAT strategy for blend lubrication would allow direct monitoring and potential control of blend lubrication and lubrication-dependent quality parameters effectively preventing over-lubrication phenomena. Monitoring strategies of the lubricant concentration have only been suggested in few studies (Aguirre-Mendez and Romañach 2007; Cameron and Briens 2019a; Cameron and Briens 2019b; Crouter and Briens 2016; Duong et al. 2003; Ebube et al. 1998). Process analytical tools to assess varying shear exposure are even less commonly investigated. Thermal effusivity (Nakagawa et al. 2013; Uchiyama et al. 2014; Yoshihashi et al. 2013) and NIR reflectance spectroscopy (Abe and Otsuka 2012; Nakagawa et al. 2013; Otsuka and Yamane 2009) have been proposed to monitor shear dependent lubrication of blends. NIR reflectance spectroscopy has also been suggested as a PAT tool to measure the shear-dependent changes in tablet the breaking force (Otsuka and Yamane 2006; Otsuka and Yamane 2009).

The non-destructive, non-ionising nature of the electromagnetic radiation used (60 GHz – 4 THz = 2 – 130 cm^{-1}) and the fast acquisition rates (sub-second) make THz-TDS ideal for PAT applications. The technique can be used in transmission and reflection mode (Zeitler et al. 2010). As many pharmaceutical materials show a high transmittance at terahertz frequencies, even rather thick or dense samples can be probed in transmission. Further, most polymeric materials are at least semi-transparent, enabling measurement through container walls (Zeitler et al. 2010). These features enabled transmission measurements of blends through a blending container in a previous study (Anuschek et al. 2024a). As THz-TDS records the signal in the time-domain, extraction of the absorption coefficient and the refractive index is possible without using complex physical models, such as the Kramers-Kronig relations (Markl et al. 2017). Numerous studies have demonstrated the correlation of the refractive index with material density, including materials such as pharmaceutical tablets and powders, in both transmission (Bawuah et al. 2021; Anuschek et al. 2024a) and reflection (Anuschek et al. 2023; Stranzinger et al. 2019).

The presented study evaluates the suitability of THz-TDS in determining blend density for monitoring the shear-dependent lubrication with MgSt by variation of the blending time. This ultimately aims to establish a monitoring strategy based on THz-TDS primarily for shear-dependent lubrication and its effect on tablet quality.

2. Materials and methods

2.1. Materials

In this study microcrystalline cellulose (MCC) (Avicel pH 200, FMC, Philadelphia, PA, USA) and magnesium stearate (MgSt) (Peter Greven, Bad Münstereifel, Germany) were used.

2.2. Blending

MCC and MgSt were blended in 100 ml high-density polyethylene (HDPE) containers (Duma®, Gerresheimer, Düsseldorf, Germany) at 25 rpm in a SentroBlender (Sentronic, Dresden, Germany) with MgSt concentrations of 0.3, 0.7, or 1.0 % (*w/w*). The containers were filled to a filling level of approximately 80 %, corresponding to 28 g of powder. During blending, the HDPE container's bottom-to-top axis was oriented perpendicular to the blending axis. The blending time was varied and is detailed in Section 2.8.1.

2.3. Untapped and tapped bulk densities

The untapped and tapped bulk densities were analysed in a 10 mL graduated cylinder with a target sample mass of 3 g (replicates = 3). The tapped bulk density was measured with a settling device (Erweka SVM Tapped Density Tester, Langen, Germany). Tapped bulk density was determined based on the minimum constant volume after 2500–3750 taps. The step changes followed the procedure described in the United States Pharmacopoeia Monograph ⟨616⟩.

2.4. Tablet manufacturing

Tablets were compressed on the Korsch XP1 (Korsch, Berlin, Germany) using an asymmetrical compression profile without pre-compression. The blends were manually weighed (200 mg target mass), filled into the die, and compressed with 10 mm flat-faced plain tooling to target porosities of 10, 15, 20, 25, and 30 %. The compression pressure was adjusted manually to reach the target porosities. The final choice of compression pressure was based on at-line measurement of tablet dimensions with a calliper (Model number: 547 – 301, Mitutoyo Europe GmbH, Neuss, Germany). Table 1 summarises the produced tablet batches.

2.5. Tablet mass, height, and diameter determination

Tablet mass, height, and diameter were determined using a ST50 tablet hardness tester (Sotax, Aesch, Switzerland). Measurements were performed one day after the THz-TDS measurements and three days after compression. The obtained values for tablet mass, height, and diameter for Batches A0-D4 (see Table 1) are summarised in Supplementary Tables S1-S4.

2.6. Porosity determination

Pycnometric density (ρ_{pyc}) was obtained from measurements of MCC (replicates = 3) using an Accupyc 1300 pycnometer (Micromeritics, Norcross, GA, USA). Samples were weighed and placed into a 1 cm^3 cup. The sample chamber was pressurised 30 times to 10 bar with helium. The nominal tablet porosity ($f_{nominal}$) was determined based on Equation (1).

$$f_{nominal} = 100\left(1 - \frac{m}{\pi\left(\frac{D}{2}\right)^2 H \rho_{pyc}}\right), \quad (1)$$

where m is the tablet mass, D is the tablet diameter, H is the tablet height, and ρ_{pyc} is the pycnometric density and all in SI units. The true density of the blends was calculated as the mass weighted harmonic mean of the true density of the individual components, i.e. MCC and

Table 1
Summary of tablet batches based on the MgSt concentration, blending time, and target tablet porosity.

Batch	MgSt concentration (%, *w/w*)	Blending time (min)	Target tablet porosity (%)
A0	0	0	10, 15, 20, 25, 30
B1	0.3	5	10, 15, 20, 25, 30
B2	0.3	10	10, 15, 20, 25, 30
B3	0.3	15	10, 15, 20, 25, 30
B4	0.3	20	10, 15, 20, 25, 30
C1	0.7	5	10, 15, 20, 25, 30
C2	0.7	10	10, 15, 20, 25, 30
C3	0.7	15	10, 15, 20, 25, 30
C4	0.7	20	10, 15, 20, 25, 30
D1	1.0	5	10, 15, 20, 25, 30
D2	1.0	10	10, 15, 20, 25, 30
D3	1.0	15	10, 15, 20, 25, 30
D4	1.0	20	10, 15, 20, 25, 30

MgSt. The obtained values for tablet porosity for Batches A0-D4 (see Table 1) are summarised in Supplementary Tables S1-S4.

2.7. Tensile strength

The ST50 tablet hardness tester (Sotax, Aesch, Switzerland) was used for breaking force measurements. The jaw movement was kept at a constant speed of 1.20 mm s^{-1}. The tensile strength (σ) was calculated with Equation (2) as described in Fell and Newton (1970),

$$\sigma = \frac{2\,BF}{DH\pi}, \tag{2}$$

where BF is the breaking force, D is the tablet diameter, and H is the tablet height and all in SI units. The measurement was performed one day after the THz-TDS measurements and three days after compression. The obtained values for tablet tensile strength for Batches A0-D4 (see Table 1) are summarised in Supplementary Tables S1-S4.

2.8. Terahertz time-domain spectroscopy

THz-TDS acquisition was performed with the TeraPulse Lx (TeraView Ltd., Cambridge, UK) in combination with a transmission chamber (Lx sample chamber, TeraView Ltd., Cambridge, UK). Before each acquisition a reference measurement of the empty chamber was acquired. Ten waveforms were averaged for each acquisition at an acquisition rate of 10 Hz. Thus, the total measurement time sums up to 1 s per THz-TDS acquisition. The experimental setup for blend and tablet measurements is illustrated in Fig. 1.

2.9. Blends

THz-TDS measurements of the blends were carried out with the blend in the HDPE container and thus measured through the HDPE container (in transmission). The position of the measurement was approximately 1 cm above the container's bottom. For each blend, reference measurements of the empty HDPE containers were acquired prior to blending.

Measurement of finished blends: Uninterrupted blending with each of the MgSt concentrations was performed in triplicates for 5, 10, 15, and 20 min subtracting 10 rotations (= 24 s). Each triplicate blend was then measured ten times. Between each of the measurement acquisitions, the container was reinstalled in the blender and the blend was mixed for one rotation using the same settings as described in Section 2.2.

Mimicked in-line measurement throughout the blending process: To investigate the continuous change in the THz-TDS response with the blending time, blends of different MgSt concentration were prepared and blended for 20 min. A THz-TDS waveform was taken before the start of the blending process. After each fifth rotation, the container was removed from the blender, a single THz-TDS waveform was acquired, the container was reinstalled, and the blending cycle was continued. This aimed to mimic an in-line measurement.

The refractive index (n) of the blends was calculated with Equation (3),

$$n(\nu) = \frac{c\Delta\Phi(\nu)}{2\pi\nu l}, \tag{3}$$

where l is the sample thickness, c is the speed of light in vacuum, ν is the frequency, and $\Delta\Phi$ is the phase difference and all in SI units. For the sample thickness, the diameter of 4.5 cm of the HDPE container was

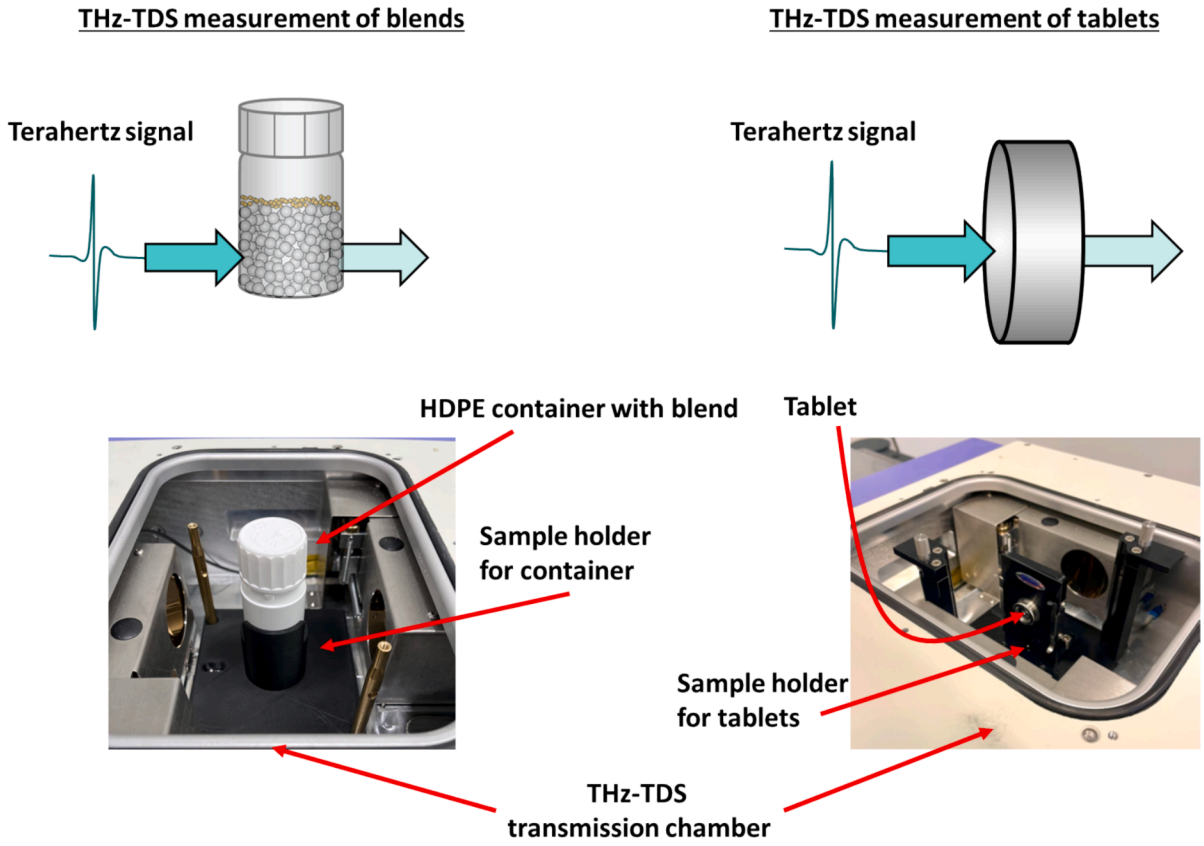

Fig. 1. Experimental setup for the THz-TDS measurement of blends (left) and tablets (right). Blends were measured in the HDPE container and thus, through container walls and the bulk of the blend. Containers were fixated with a 3D printed sample holder. Tablets were measured along the axial dimension and through the centre of the tablet. Tablets were fixated with a sample holder provided by the manufacturer of the THz-TDS equipment.

used. To account for both variances in the laser intensity and the HDPE containers, the total phase difference of the blend was calculated after Equation (4),

$$\Delta\Phi(\nu) = \left[\Phi_{\text{Blend}}(\nu) - \Phi_{\text{R, Blend}}(\nu)\right] - \left[\Phi_{\text{HDPE}}(\nu) - \Phi_{\text{R, HDPE}}(\nu)\right], \quad (4)$$

where Φ_{HDPE} and Φ_{Blend} are the measured phase of the empty HDPE container and the container with the blend, respectively, $\Phi_{\text{R,HDPE}}$ and $\Phi_{\text{R,Blend}}$ are the references measured in an empty chamber prior to container and blend acquisition, respectively, and ν is the frequency and all in SI units. The reference measurements through the empty chamber accounted for laser fluctuations and drifts. It is noted that these primarily affect the signal amplitude rather than the time-delay and are thus not considered necessary in future applications if only the refractive index is investigated.

2.10. Tablets

Spectra of the tablets were acquired in transmission by fixating the tablet in the focus of the beam so that the centre of the face of the flat-faced tablet was probed. The refractive index of the tablet was calculated with Equation (3) where the sample thickness was replaced with the tablet height. The phase difference was calculated using Equation (5),

$$\Delta\Phi(\nu) = \left[\Phi_{\text{Tablet}}(\nu) - \Phi_{\text{R, Tablet}}(\nu)\right], \quad (5)$$

where Φ_{Tablet} and $\Phi_{\text{R,Tablet}}$ are the measured phase of the tablet and the references measured in an empty chamber and ν is the frequency and all in SI units.

2.11. Data processing

Data processing was performed with Matlab R2021a (MathWorks, Natick, MA, USA). The statistical analysis for the ANOVA model was performed with JMP 16 (JMP Statistical Discovery LLC, Cary, NA, USA).

The root mean squared error (RMSE), and adjusted root mean squared error (RMSE_{adj}) were used for model evaluation and calculated as

$$\text{RMSE} = \sqrt{\frac{\sum_{i=1}^{N}(y_i - y_c)^2}{N}}, \quad (6)$$

$$\text{RMSE}_{\text{adj}} = \sqrt{\frac{\sum_{i=1}^{N}(y_i - y_c)^2}{N - p}}, \quad (7)$$

where y_i denotes the measured value of sample i, y_c denotes the predicted value, N denotes the total number of measurements, and p denotes the number of coefficients in the model.

The moving block standard deviation (MBSD) of the refractive index for the mimicked in-line measurement was calculated as

$$\text{MBSD}_k = \sqrt{\frac{\sum_{k}^{i=k+(N_B-1)}(n_i - \overline{n_k})^2}{N_B - 1}}, \quad (8)$$

where i denotes the number of the measurement in the time series, k denotes the number of the block in the time series, N_B the block size, n_i the refractive index of the ith measurement in the time series used in the kth block, and n_k ¯ the averaged refractive index of block k. In each new block, only the succeeding measurement point in the time series data is added, while the first measurement point from the previous block is excluded.

3. Results and discussion

3.1. Investigation of blends

Mixtures with MCC and different concentrations of MgSt (0.3, 0.7, and 1.0 %) were exposed to different levels of shear by extending the blending time (5, 10, 15, and 20 min). Increased blending times systematically shifted the untapped bulk density towards higher values (Fig. 2). The same effect was observed for increased MgSt concentrations. This agrees with previous results showing that increased MgSt concentration and increased shear exposure of the particles results in a densification of the powder bed (Shah and Mlodozeniec 1977; Danser-eau and Peck 1987; Mehrotra et al. 2007; Kushner IV 2012). This behaviour is a result of the reduced friction between particles, and thus improved powder flowability and denser packing of the powder. In contrast, tapping ultimately forces the powder to pack at maximum density, irrespective of the particle friction. This caused the less distinct trend in the tapped bulk density in Fig. 2, though the data suggests that at least compared to MCC alone, addition of MgSt increased the tapped bulk density.

The suitability of HDPE as a container material for THz-TDS measurements on powders is described elsewhere (Anuschek et al. 2024a). Between each of the ten measurements, the blend was reinstalled in the blender and rotated for a single rotation. The single rotation of the blend container included between measurements served two purposes: firstly, to simulate a dynamic measurement of the blend at the end of a blending cycle, and secondly to minimise the risk that the densified state of the blend was biased due to the transferring between blender and THz-TDS apparatus. The refractive index was analysed instead of, e.g. the absorption coefficient or the time-domain data, due to its well-described correlation with material density at terahertz frequencies (Bawuah et al. 2021; Stranzinger et al. 2019). The refractive index at 0.25 THz was used for the analysis as the sample thickness limited the dynamic range towards higher frequencies (see Supplementary Figs. S1 – S3).

Fig. 3 illustrates the measured refractive index (n_{Blend}) as a function of the untapped bulk density. The small sample size used for bulk density measurements caused a high variation. Nonetheless, the refractive index visibly correlated with the measured untapped bulk density regardless of the used MgSt concentration. As no conclusive additional effect of MgSt concentration on the refractive index was observed, it is suggested that the contribution of MgSt to the measured refractive index was negligible compared to the effect of powder densification.

A close to linear trend of the refractive index with the blending time was found for the three MgSt concentrations when excluding the MCC sample from the fit (Fig. 4). Within the investigated blending timeframe,

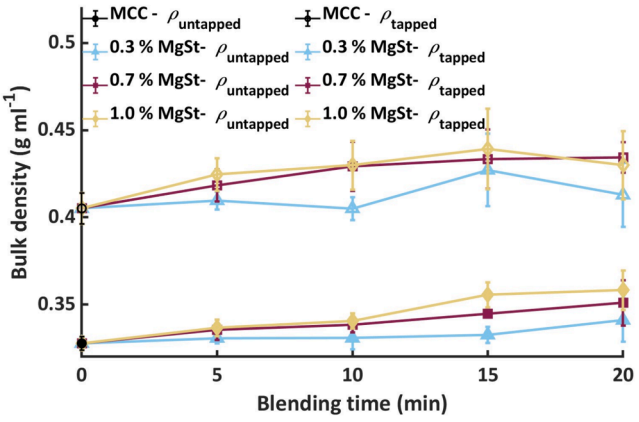

Fig. 2. Averaged untapped (ρ_{untapped}) and tapped (ρ_{tapped}) bulk densities (replicates = 3) for MCC and for blends of MCC with 0.3, 0.7, and 1.0 % MgSt as a function of blending time. The error bars indicate the standard deviation for the triplicates.

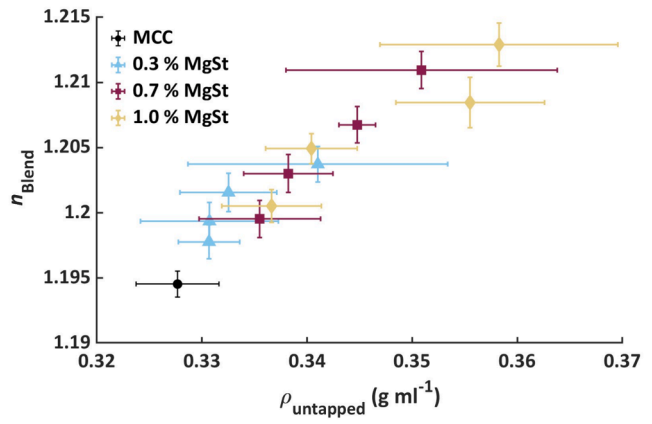

Fig. 3. Averaged refractive index (n_{Blend}) (replicates = 10 each on 3 samples) at 0.25 THz as a function of the averaged untapped bulk density ($\rho_{untapped}$) (replicates = 3) for MCC and for blends of MCC with 0.3, 0.7, and 1.0 % MgSt blended for 5, 10, 15, and 20 min. The error bars of $\rho_{untapped}$ indicate the standard deviation for the triplicates. The error bars of n_{Blend} indicate the pooled standard deviation of the ten measurements taken for each triplicate.

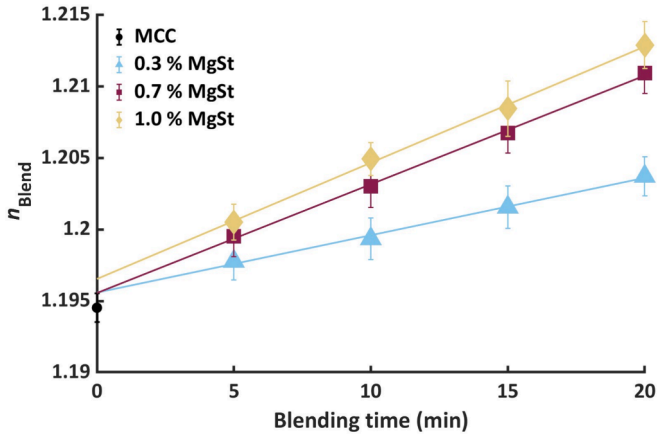

Fig. 4. Averaged refractive index (n_{Blend}) at 0.25 THz (replicates = 10 each on 3 samples) for MCC and for blends of MCC with 0.3, 0.7, and 1.0 % MgSt as a function of blending time. The error bars indicate the pooled standard deviation of the ten measurements taken for each triplicate. The solid lines are the linear fitting functions.

the gradient of the linear fit increased with the MgSt concentration, reaching values of 0.40, 0.76, and 0.81 min^{-1} with RMSEs of 0.0066, 0.011, and 0.013 for the blends containing 0.3, 0.7, and 1.0 %, respectively. With increased MgSt concentration, the blend thus densified more effectively, rendering the refractive index more sensitive to changes in the blending time (i.e. shear exposure). As the linear fits did not intercept at the refractive index of MCC, an initial, non-linear phase during blending is suggested, in which the MgSt particles were distributed until macrohomogeneity was reached. In addition, it is expected that with increased blending times, the observed linear trend will level out as a maximum surface coverage of MgSt is reached. Similar observations are reported for thermal effusivity monitoring (Nakagawa et al. 2013) or the tensile strength (Kushner IV and Moore 2010; Kushner IV 2012). The refractive index for MCC alone was in good agreement with values found in Anuschek et al. (2024a), despite the difference in diameter of the blending container used (4.5 cm in the presented results versus 3.6 cm in Anuschek et al. (2024a)). This showcases the robustness of THz-TDS-based refractive index measurements for particulate systems. Comparing the blending trends in Fig. 4 with that shown in Fig. 2 suggests that THz-TDS is a more sensitive approach for evaluating density changes compared to untapped bulk density measurements. Though larger sample sizes would most likely have resulted in a more robust determination of the bulk densities, such an approach is considered impractical for a frequent, in-process evaluation.

3.2. Investigation of tablets

The different blends were compressed to tablets at five target porosities (see Table 1 and Supplementary Tables S1-S4) and subsequently subjected to THz-TDS transmission measurements to examine the impact of MgSt concentration and shear-exposure due to different blending times on the refractive index after compression. It is noted that tablets of unlubricated MCC were consistently produced with lower porosities. This could be a result of enhanced elastic recovery of lubricated tablets as described by Zuurman et al. (1999). However, this observation is not considered relevant within the context of this study and is thus not further addressed. The refractive index spectra are shown in Supplementary Figures S4 – S7. To select a frequency for the refractive index analysis, the coefficient of determination (R^2) of a linear fit of refractive index and porosity was determined as a function of the frequency (see Supplementary Fig. S8). This approach has previously been used by Skelbæk-Pedersen et al. (2020) and is based on a generally close to linear relation between the refractive index and tablet porosity (Bawuah et al. 2020). As R^2 seemed unaffected in the range of 0.2 to 1.5 THz with values consistently high around 0.99, the refractive index was averaged in the frequency range from 0.4 to 0.8 THz, a commonly used range for tablet analysis (Bawuah et al. 2020).

The averaged refractive index (n_{Tablet}) of the tablets correlated linearly with tablet porosity ($f_{nominal}$) independent of the blend composition and blending time (Fig. 5). This confirms that the dependency of the refractive index on the untapped bulk density in Fig. 3 was in fact the result of blending time-dependent densification of the powder. Any additional contribution of MgSt to the spectrum of, e.g. the crystal phonon modes, would have been visible even after compression to a defined density if present.

3.3. Process monitoring of blending with MgSt

To investigate whether monitoring of density changes with THz-TDS can be used to control blend lubrication with MgSt, an in-line measurement of the blend was mimicked. The blend was measured through the container at every fifth rotation for a total blending time of 20 min. In addition, a single measurement of the powder was acquired before the start of the blending cycle. The refractive index as a function of blending

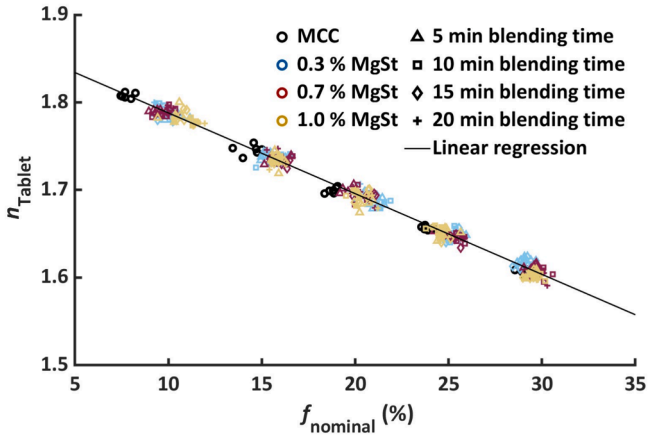

Fig. 5. Refractive index of tablets (n_{Tablet}) averaged between 0.4 and 0.8 THz as a function of the nominal tablet porosity ($f_{nominal}$) for tablets prepared from MCC and from blends of MCC with 0.3, 0.7, and 1.0 % MgSt blended for 5, 10, 15, and 20 min. The solid line is the linear fitting function.

time can be found in Fig. 6 (top). The refractive index at 0.25 THz was extracted for the analysis in alignment with Section 3.1 (for refractive index spectra see Supplementary Figs. S9 – S11). The mimicked in-line acquisition during the blending cycle mirrored the previously obtained results on the finished blends (Fig. 4). A predominantly linear increase of the refractive index with the blending time was found, indicating a continuous densification of the blend. However, within the first five rotations this increase deviated from the linear trend. MgSt seemingly caused an almost instantaneous, within a few rotations, increase in the blend density. Using the previous linear fitting functions obtained from the finished blends (Fig. 4), overall, slightly higher values were found for the mimicked in-line measured blends, yielding root mean squared errors for the refractive index of 0.0013, 0.0011, and 0.0016 for blends with 0.3, 0.7, and 1.0 %, respectively (Fig. 6 top). To investigate this further, the corresponding blending times of the in-line measurements were predicted based on the refractive index and the linear models established in Fig. 4 as shown in Fig. 6 (bottom). Initially, the models accurately predicted the blending times but deviated towards higher values after around 10 min. The deviation is attributed to the difference in the blending dynamics of the non-interrupted blending process in the analysis of the finished blends, and the frequently interrupted, mimicked in-line blending process. Especially, the frequent sample transfer between blender and THz-TDS equipment, could have resulted in increased shear exposure or tapping densification of the blends. This is aligned with the increasingly deviating predictions at longer blending times, for which the accumulating number of sample transfers could have caused a continuous increase in the excess shear or tapping of the system and, thus, powder density. Such differences in the THz-TDS results of these two measurement modes (non-interrupted blending and interrupted blending by mimicking in-line measurements) have also been described previously by Anuschek et al. (2024a) for the investigation of blending processes. In addition, the frequent sample transfers between THz-TDS measurement chamber and blender are expected to have resulted in additional variation of the measurements, which is expected to improve if a real in-line setup is used. However, as also in such a setup density-fluctuations can be expected, Fig. 6 demonstrates that systematic changes in density due to MgSt can be followed even in the presence of density-fluctuations by following the magnitude of the systematic changes.

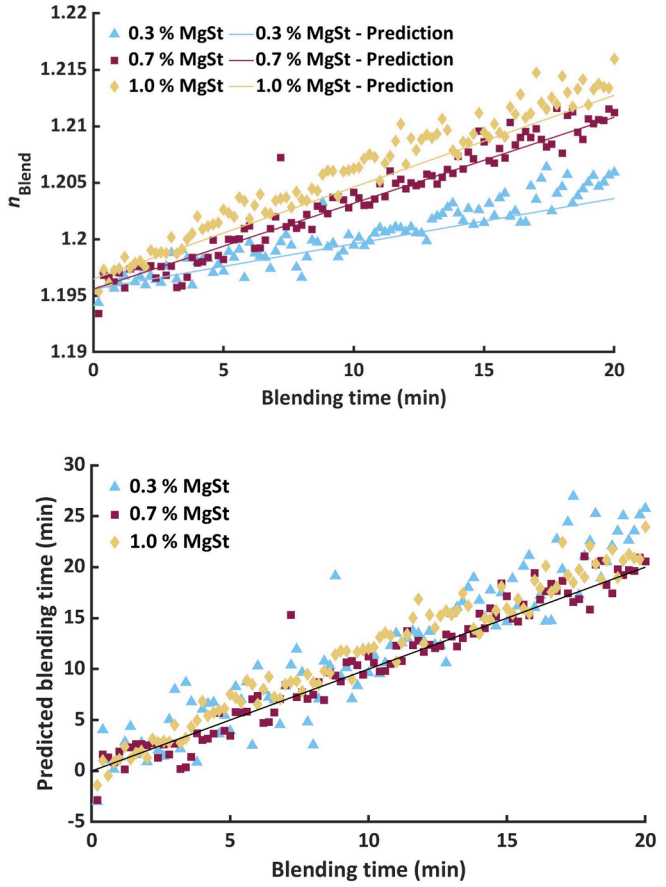

Fig. 6. Top: refractive index of blends (n_{Blend}) of blends of MCC with 0.3, 0.7, and 1.0 % MgSt as a function of blending time during the mimicked in-line blending. The solid lines are the linear fitting functions obtained from the finished blends (Section 3.1). Bottom: predicted blending time based on the linear fitting functions for the finished blends in Fig. 4 and the refractive index obtained during the mimicked in-line blending and shown as a function of the actual blending time for the mimicked in-line blending for blends of MCC with 0.3, 0.7, and 1.0 % MgSt. The straight line is the bisector.

4. Considerations for process integration of THz-TDS for monitoring shear-dependent lubrication

4.1. General considerations

A general suggestion for THz-TDS based powder monitoring for batch and continuous manufacturing processes can be found in Anuschek et al. (2024a). Monitoring of shear-induced lubrication, as described in this work, may require some additional considerations. Rate of change models, such as the moving block standard deviation (MBSD) or moving F-test, are commonly applied in blend monitoring strategies (Besseling et al. 2015; FDA 2021). However, they cannot be applied to the presented THz-TDS analysis to monitor lubrication. This is demonstrated with the MBSD as a function of the blending time in Supplementary Fig. S12 using a block size of ten. Similar values were found between the three MgSt concentrations with a constant range of values for the whole blending process. The result was expected as THz-TDS follows the lubrication process as a function of the physical density changes and not the homogeneous chemical distribution of MgSt in the blend.

Instead, an endpoint or steady-state could be defined by a target density monitored with THz-TDS, for which the manufacturability of the powder and its favourable tablet properties have been proven. A predictive model could also directly be applied for which the impact of lubrication extent based on the measured density is related to a target CQA (see Section 3.4.3). Both require positioning of the probe at a location in the process where the powder can settle or flow in a controlled manner. If strong density fluctuations are observed, monitoring of the moving block average should be considered, to follow an underlying trend. Positioning the probe as close to tablet compression as possible would enable the monitoring of the lubricated blend after the additional shear introduced in total by all the various process steps. For example, the tableting feed frame would be well suited for sample presentation. However, with such a positioning it would be too late to react to an unacceptable blend without needing to discard blend to waste and earlier positions in the production process may therefore be more desirable. For in-line measurements, variation in blend density unrelated to lubrication should be considered when deciding on the probe position. Finally, changes in raw material attributes, e.g. water content or particle size and morphology distributions, may affect the measured refractive index and should be considered during development, validation, and throughout the lifecycle of the analytical procedure.

The presented strategy is considered particularly advantageous during continuous manufacturing where real-time assessment of formulation properties is necessary to ensure a state of control throughout the manufacturing process. However, as shear variability in blend intermediate may vary from batch to batch, THz-TDS as a fast and non-destructive method to assess such variability could also be considered within batch processes. Once variability in process or on the batch are detected, corrective actions can be taken within an established

framework for feedback (e.g. adjustment of blend parameters) and feed forward (e.g. adjustment of tablet porosity) process control.

It should be noted that a final monitoring strategy is not expected to require reference measurements before each measurement as performed in the presented study. Also, the measurement time of 1 s can be shortened if desired. By adjusting the probed time window, measurement rates of up to 50 measurements/s can be achieved, which could reduce the measurement time towards one fifth. Faster measurement rates could be acceptable as it has been shown to only have limited effects on the accuracy of time delay related parameters (Anuschek et al. 2024b).

4.2. Comparison of THz-TDS to proposed alternative methods for MgSt-blend analysis

Using density changes of blends containing MgSt to monitor blend lubrication has also been suggested using thermal effusivity and NIR reflectance spectroscopy (Uchiyama et al. 2014; Yoshihashi et al. 2013; Nakagawa et al. 2013). The advantage of one PAT tool over the other will likely be a combination of factors. In comparison to thermal effusivity and NIR reflectance spectroscopy, THz-TDS has the advantage of a well-described and clear dependency between the refractive index at terahertz frequencies and material density for which various physical models have been demonstrated (Bawuah et al. 2020). These models commonly depend on the pore and particle shape besides the powder or compact density. However, as pores or particle shapes are not likely to change upon blending, the density can be considered the main contributor to changes in the refractive index. Further, a linear fitting function is a sufficiently good approximation for most cases, although more complicated underlying models can be assumed. In comparison, thermal effusivity is determined by three separate variables, namely the thermal conductivity, heat capacity, and powder density, all of which might change during a blending process (Uchiyama et al. 2014). Uchiyama et al. (2014) demonstrated that a correlation between thermal effusivity and bulk density can only be established once thermal conductivity and heat capacity stabilise. The sensitivity of NIR spectroscopy to physical parameters of the sample is often complex and a result of differences in the diffused scattering behaviour and changes in the effective path length of the radiation in the sample (Otsuka and Yamane, 2006). Based on this, some studies have investigated the applicability of NIR reflectance measurements to monitor blending dynamics of lubricated powders (Nakagawa et al. 2013; Otsuka and Yamane 2006; Otsuka and Yamane 2009). Compared to THz-TDS transmission measurements, NIR reflectance spectroscopy may offer the opportunity to simultaneously monitor the chemical composition of the blend and thus MgSt concentration. However, density changes might affect the accuracy of the concentration monitoring as they may be confounded, in particular at low concentrations. As changes in the MgSt concentration could not be assessed with THz-TDS, a joined monitoring strategy could be considered. In combination with THz-TDS, that would monitor shear-exposure based on density changes, a second process analyser, which is proven sensitive to the MgSt concentration (i.e. NIR reflectance or Raman spectroscopy), could be implemented for an accurate monitoring of the lubrication of the blend. A comparable strategy was also proposed by Nakagawa et al. (2013) using thermal effusivity and NIR reflectance spectroscopy. However, THz-TDS does not require direct contact with the sample in contrast to thermal effusivity measurements.

4.3. Case study: A THz-TDS-based model to predict the tensile strength

In the following, a case study is presented of how THz-TDS monitoring of shear exposure of MgSt containing systems could be included into a monitoring approach of CQAs sensitive to lubrication. The tablet tensile strength was used as a CQA that is well-known to be affected by the shear exposure of MgSt containing blends. Commonly, a reduction in tensile strength upon increased shear exposure is explained by an expanding surface coverage of the primary particles with MgSt and the in turn resulting decrease in particle–particle bonding strength (Shah and Mlodozeniec 1977; Wang et al. 2010). This effect is particularly pronounced in materials with ductile behaviour upon compression, e.g. MCC as used in this study. Here, fragmentation is limited and thereby the creation of new surfaces unexposed to MgSt is restricted (Jarosz and Parrott 1984).

The effect of blending time (i.e. shear), MgSt concentration, and porosity on the produced tablets is exemplified in Fig. 7. Results are presented semi-logarithmically as a function of porosity aligned with the commonly used Ryshkewitch-Duckworth equation as described in the USP monograph < 1062 > Tablet Compression Characterisation (Ryshkewitch 1953; USP 2024). However, the data deviated from the ideal, linear behaviour and a second-degree polynomial fitting function was found to describe the compactibility behaviour better. Naturally, tablet tensile strength was strongly affected by porosity as apparent in Fig. 7. A general trend towards lower tensile strengths was found with increased MgSt concentration. Similarly, the tensile strength decreased when blending was prolonged.

To incorporate THz-TDS-based monitoring of shear exposure for production of tablets into a monitoring strategy for the tensile strength, it is necessary to also consider tablet porosity and the concentration of MgSt. Given the extensive study on THz-TDS as a PAT tool for tablet porosity (Markl et al. 2017; Bawuah et al. 2020, 2021, 2023; Anuschek et al. 2023), a direct combination of the two THz-TDS-based procedures was considered reasonable. An illustration of how such a monitoring strategy could be included in a production batch process is presented in Fig. 8, where tensile strength is evaluated based on

i) THz-TDS-based monitoring of blend density relating to primarily the shear exposure based on the measured blend refractive index as presented in Section 3.1 and 3.3. It is noted that Fig. 4 demonstrates that also MgSt concentration affects the bulk density and thus a combined effect of MgSt concentration and shear is monitored.
ii) THz-TDS-based monitoring of tablet porosity based on the refractive index (see Fig. 5 in Section 3.2).
iii) The MgSt concentration in the formulation which could for example be based on the recipe, actual amounts, or additional PAT tools, e.g. NIR reflection or Raman spectroscopy.

To evaluate the potential of such a THz-TDS-based model for the tensile strength, a three-way mixed ANOVA was applied on the collected data of all produced tablet batches (see Table 1). Tablet mass,

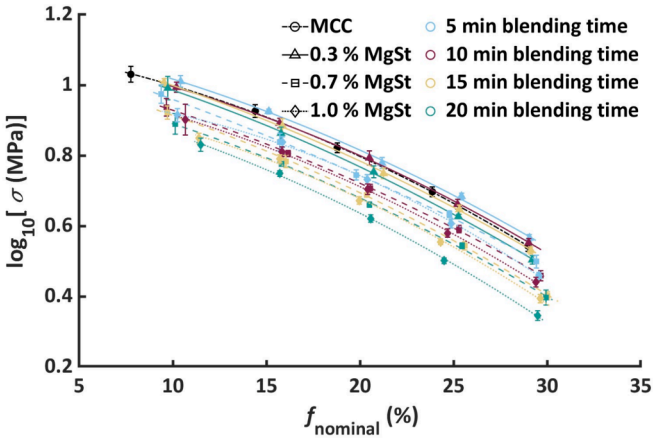

Fig. 7. The decadic logarithm of the tablets' tensile strength (σ) as a function of nominal tablet porosity ($f_{nominal}$) for tablets prepared from MCC and from blends of MCC with 0.3, 0.7, and 1.0 % MgSt blended for 5, 10, 15, and 20 min. The lines are the second-degree polynomial fits.

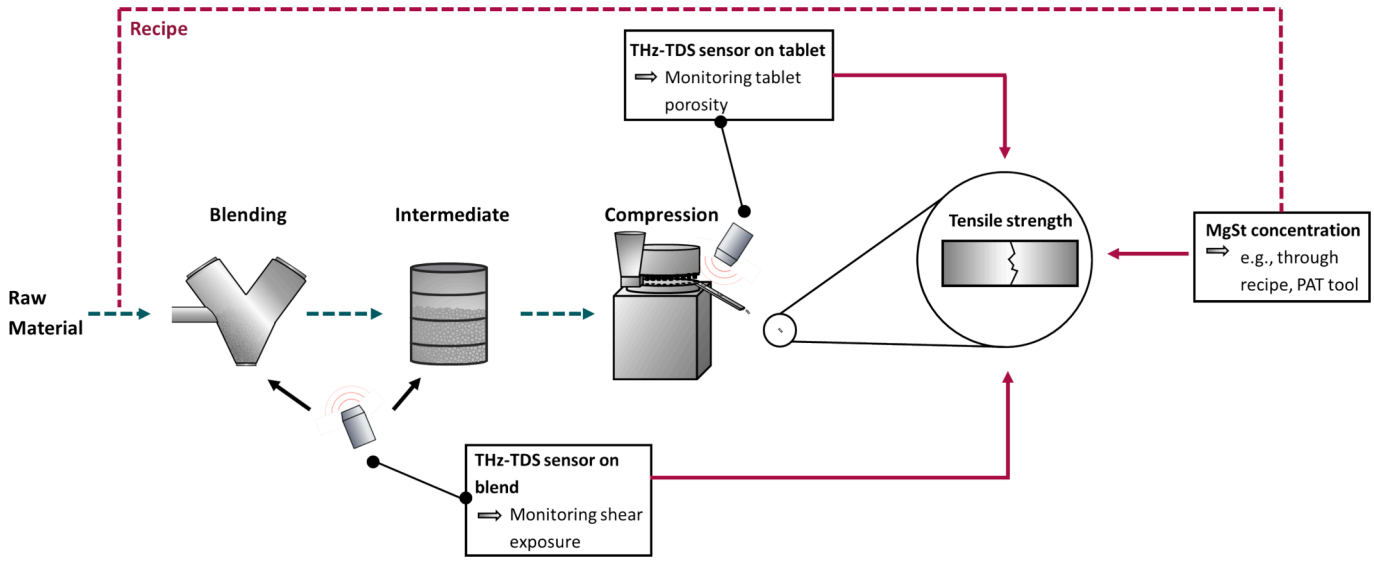

Fig. 8. Illustration of the envisioned control strategy within a batch process. A first THz-TDS sensor assesses the blend density, i.e. lubrication-dependent blend densification to primarily assess the shear exposure, either during/after the blending step or after storage of the blend intermediate. A second THz-TDS sensor assesses tablet porosity after compression. Input from both models is combined with the MgSt concentration (e.g. based on recipe or other PAT tools) to predict the effect on the tablet tensile strength according to Equation (9), or other tablet CQAs.

dimensions, porosity, and tensile strength are summarised in Supplementary Tables S1-S4. The MgSt concentration, the refractive index of the blend (as a surrogate for blending time i.e. shear, see Fig. 4), and the refractive index of the tablets (as a surrogate for porosity, see Fig. 5) were included as factors to describe the logarithmic tensile strength. The logarithmic tensile strength was used due to the linear relation when applying the Ryshkewitch-Duckworth equation. The three main factors, the self-interaction of the refractive index of the tablets and of the MgSt concentration (quadratic terms), and the interaction between the refractive index of the tablets and the MgSt concentration were found to influence the logarithmic tensile strength significantly. To avoid overfitting, the effect of each factor on the root mean squared error of the models adjusted for the number of fitting parameters ($RMSE_{adj}$) was investigated. The resulting model comprised the three main factors and the self-interaction of the refractive index of the tablets (Equation (9), $p = 0.0001$, $RMSE_{adj} = 0.021$),

$$\log_{10}(\sigma) = -7.79n_{Blend} + 16.5n_{Tablet} - 4.09n_{Tablet}^2 - 0.07w_{MgSt} - 6.10\text{MPa} \quad (9)$$

where σ is the tensile strength, w_{MgSt} is the MgSt concentration, and n_{Blend} and n_{Tablet} are the refractive index of the blend and tablet, respectively. Coefficients in Equation (9) are not normalised to enable direct prediction of the tensile strength based on non-adjusted input parameters. Normalisation resulted in coefficients of −0.067, 0.29, −0.066, −0.055, for n_{Blend}, n_{Tablet}, n_{Tablet}^2, and w_{MgSt}, respectively. Equation (9) can be interpreted as a combined model where:

i) the first term shows a linear dependency for the logarithmic tensile strength with the blend bulk density, but with the bulk density replaced with the refractive index of the blend. The term captures changes in the tensile strength by increased blending time or MgSt concentration as shown in Fig. 4. It is noted that the effect of blending time can be more universally understood as the effect of shear on the system.
ii) the second and third terms show the almost linear dependency for the logarithmic tensile strength with the tablet porosity in accordance with the use of the Ryshkewitch-Duckworth equation. The third term can be considered a correction for the deviating, slightly curved dependency in Fig. 7, aligned with the second degree polynomial fit. In the model, the tablet porosity is replaced with the tablet refractive index based on the linear relation between refractive index and porosity for tablets in Fig. 5.
iii) the fourth term adjusts for the tensile strength dependency of the MgSt concentration in the compactibility plots (Fig. 7). This term corrects for additional changes in density due to MgSt that are not already explained by i.).

To analyse the impact of each term on the error, models based on Equation (9) were examined with specific terms removed. The corresponding RMSEs are summarised in Table 2. When including only tablet porosity (i.e., n_{tablet}) in the model, the error more than doubled. However, a noticeable reduction in error was achieved by incorporating n_{Blend}. The inclusion of n_{Blend}, which captures blending time and MgSt-related changes, reduced the RMSE by 46 %. Additional inclusion of w_{MgSt} further reduced the error though the term only corrects the concentration-related effects that are not already captured in the density changes measured with n_{Blend}. Removing the term could be feasible but ultimately depends on the discrepancy between bulk density increase and tensile strength decrease for a given formulation when not only shear-exposure but also MgSt concentration are varied.

Cross-validation results of the model are shown in Fig. 9 as the predicted versus measured tensile strength within the 10-fold cross-validation. Larger deviations were found towards higher values and, therefore, also with decreased MgSt concentrations. This should not be attributed to variations from the THz-TDS measurements but rather to the variations in the breaking force determination, which increased with the breaking forces. This is evident based on the variations depicted as error bars in Fig. 9, which are the standard deviation of the tensile strength for tablets of the same porosity, blending time, and MgSt concentration (replicates = 6). The variation in tensile strength mirrored the variation in its prediction, showcasing that the increased errors at higher

Table 2
Root mean squared errors (RMSE) for different fitting models based on Equation (9). The error is shown for the predicted tensile strength (non-logarithmic form).

Factors included	As Equation (9)	n_{Tablet}, n_{Tablet}^2	n_{Blend}, n_{Tablet}, n_{Tablet}^2
RMSE (MPa)	0.30	0.75	0.41

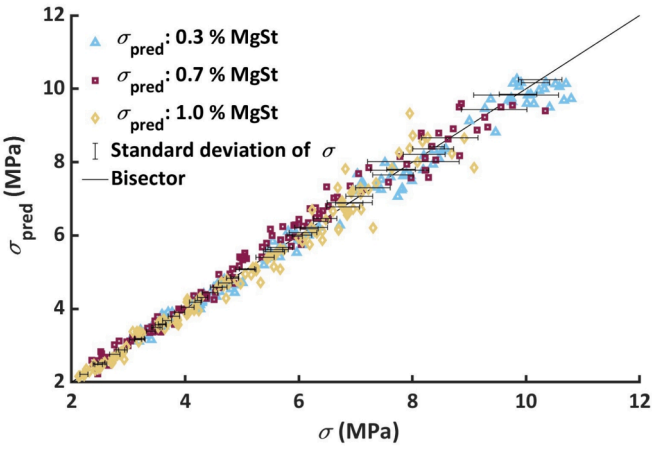

Fig. 9. Predicted tensile strength (σ_{pred}) as a function of the actual tensile strength (σ) for tablets prepared from blends of MCC with 0.3, 0.7, and 1.0 % MgSt blended for 5, 10, 15, and 20 min. The error bars indicate the standard deviation of the actual tensile strength measurements (replicates = 6).

values originate primarily from the breaking force method itself.

The developed model was further applied to the mimicked, in-line measurements of the blending process. The in-line measured refractive index of the blends, the MgSt concentration, and the measured refractive index of the respective tablets compressed to 20 % porosity (as an example target porosity), served as input parameters for the model (Equation (9). Naturally, an increased blending time or MgSt concentration caused a decrease in the predicted tensile strength (Fig. 10). Conversion of data collected during the process or blend intermediate batches after storage can therefore aid in assessing the impact of the extent of shear-exposure on lubrication dependent quality attributes.

It is therefore concluded that a combined THz-TDS measurement strategy to assess the effect of MgSt, particularly related to shear (here varied by changes in the blending time) and tablet porosity for tensile strength monitoring as outlined in Fig. 8 is generally feasible. It demonstrates the potential to monitor lubrication, including shear-related effects, of the blend as well as its influence on drug product quality. This approach may possibly also translate to other lubrication-dependent CQAs, such as friability, disintegration time, or dissolution performance. Further, a translation to a continuous setup could be envisioned in which THz-TDS sensor placement would follow the suggestions in Section 3.4.1. The needed input for MgSt concentration could be based on suitable process analysers (e.g. NIR reflection or Raman spectroscopy) or alternatively feeder data. With regards to the specific aim of monitoring the effect on the tensile strength, implementation of the proposed analytical procedure, would also allow a more detailed control of the compression step. State-of-the-art, real-time control strategies of tablet compression are based on an automated, routine assessment of tablet breaking force and mass (Markl et al. 2020; Singh et al. 2014). A variation of MgSt concentration or shear-exposure of the lubricated blend would likely be reflected in the automated breaking force assessment. However, such changes in the breaking force would trigger an erroneous adjustment of the tableting process, i.e. increased shear exposure would result in a reduced tensile strength/breaking force, triggering an increase in the compression pressure. As a result, disintegration and dissolution properties of the tablets would be altered twice – by increased lubrication of the blend and decreased porosity of the compact. Thus, incorporating a PAT strategy for blend lubrication would not only allow direct monitoring and potential control of blend lubrication and of lubrication-dependent quality parameters, thus effectively preventing over-lubrication phenomena, but also result in overall increased process control capabilities.

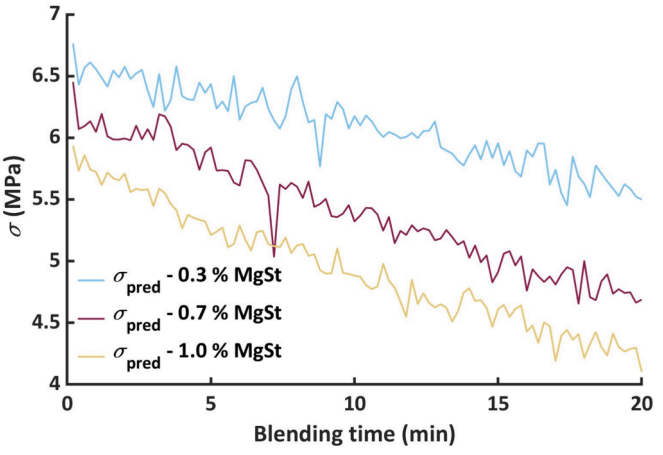

Fig. 10. The predicted tensile strength of tablets at 20 % target porosity as a function of blending time for blends with MCC and 0.3, 0.7, and 1.0 % MgSt. The tensile strength was predicted according to Equation (9) using the actual refractive indices obtained during the interrupted blending time, the nominal MgSt concentration, and the refractive index of the respective tablets at 20 % porosity.

5. Conclusion

The presented study investigated the applicability of THz-TDS as a process analyser for monitoring shear-dependent lubrication of MgSt-containing blends. It was demonstrated that the change in blend density upon increased blending times can be assessed based on the refractive index of the blend measured with THz-TDS. A linear increase in the refractive index with the blending time and powder density was found for blends containing 0.3, 0.7, and 1.0 % MgSt. This effect was found in finished blends and blends measured continuously over a 20 min blending cycle. It was further demonstrated that blend density measurements by THz-TDS can be used as a surrogate to evaluate the total shear-exposure. This was shown by a joint blend and tablet density measurement with THz-TDS for a predictive tensile strength model. The blend assessment primarily factored in the impact of shear exposure, while the tablet measurement considered the effect of porosity on tensile strength. Inclusion of the THz-TDS assessment of the blend density, resulted in an improved tensile strength description, reducing the RMSE by over 40 % (0.33 MPa). The promising results indicate that THz-TDS-based density monitoring is a viable method for tracking shear exposure in MgSt-containing blends and could be integrated into a PAT framework for effective process monitoring and quality control in tablet manufacturing.

CRediT authorship contribution statement

Moritz Anuschek: Writing – review & editing, Writing – original draft, Visualization, Validation, Software, Project administration, Methodology, Investigation, Formal analysis, Data curation, Conceptualization. **Thea Nilsson:** Writing – review & editing, Writing – original draft, Visualization, Validation, Software, Investigation, Formal analysis, Data curation. **Anne Linnet Skelbæk-Lorenzen:** Writing – review & editing, Supervision, Resources, Project administration, Funding acquisition. **Thomas Kvistgaard Vilhelmsen:** Writing – review & editing, Supervision, Resources, Project administration, Funding acquisition. **J.Axel Zeitler:** Writing – review & editing, Supervision, Software, Project administration. **Jukka Rantanen:** Writing – review & editing, Supervision, Resources, Project administration, Funding acquisition.

Declaration of competing interest

The authors declare that they have no known competing financial

interests or personal relationships that could have appeared to influence the work reported in this paper.

DECLARATION OF GENERATIVE AI AND AI-ASSISTED TECHNOLOGIES IN THE WRITING PROCESS

During the preparation of this work the author(s) used Chat Generative Pre-Trained Transformer (Chat GPT) by Open AI in order to improve language and readability. After using this tool, the authors reviewed and edited the content as needed and take full responsibility for the content of the publication.

Acknowledgement

Novo Nordisk A/S (Bagsværd, Denmark) has financed the PhD project of Moritz Anuschek (STAR program). Moritz Anuschek, Thea Nilsson, Anne Linnet Skelbæk-Lorenzen, and Thomas Kvistgaard Vilhelmsen are employed at Novo Nordisk A/S. Jukka Rantanen and J. Axel Zeitler have not received any consulting fees from Novo Nordisk A/S.

Appendix A. Supplementary data

Supplementary data to this article can be found online at https://doi.org/10.1016/j.ijpharm.2025.125303.

Data availability

Data will be made available on request.

References

Abe, H., Otsuka, M., 2012. Effects of Lubricant-Mixing Time on Prolongation of Dissolution Time and Its Prediction by Measuring near Infrared Spectra from Tablets. *Drug Dev. Ind. Pharm.* 38 (4), 412–449. https://doi.org/10.3109/03639045.2011.608679.

Aguirre-Mendez, C., Romañach, R.J., 2007. A Raman Spectroscopic Method to Monitor Magnesium Stearate in Blends and Tablets. *Pharm. Technol. Eur.* 19, 53–61. https://www.pharmtech.com/view/raman-spectroscopic-method-monitor-magnesium-stearate-blends-and-tablets.

Anuschek, M., Vilhelmsen, T.K., Zeitler, J.A., Rantanen, J., 2023. Towards Simultaneous Determination of Tablet Porosity and Height by Terahertz Time-Domain Reflection Spectroscopy. *Int. J. Pharm.* 646, 123424. https://doi.org/10.1016/j.ijpharm.2023.123424.

Anuschek, M., Skelbæk-Pedersen, A.L., Skibsted, E., Kvistgaard Vilhelmsen, T., Zeitler, J. A., Rantanen, J., 2024a. THz-TDS as a PAT Tool for Monitoring Blend Homogeneity in Pharmaceutical Manufacturing of Solid Oral Dosage Forms: a proof-of-concept study. *Int. J. Pharm.* 662, 124534. https://doi.org/10.1016/j.ijpharm.2024.124534.

Anuschek, M., Kvistgaard Vilhelmsen, T., Zeitler, J.A., Rantanen, J., 2024b. THz-TDS transflection measurements as a process analyser for tablet mass. *Int. J. Pharm.* 666, 124750. https://doi.org/10.1016/j.ijpharm.2024.124750.

Bawuah, P., Markl, D., Farrell, D., Evans, M., Portieri, A., Anderson, A., Goodwin, D., Lucas, R., Zeitler, J.A., 2020. Terahertz-Based Porosity Measurement of Pharmaceutical Tablets: A Tutorial. *J. Infrared Millim. Te.* 41 (4), 450–469. https://doi.org/10.1007/s10762-019-00659-0.

Bawuah, P., Markl, D., Turner, A., Evans, M., Portieri, A., Farrell, D., Lucas, R., Anderson, A., Goodwin, D.J., Zeitler, J.A., 2021. A Fast and Non-Destructive Terahertz Dissolution Assay for Immediate Release Tablets. *J. Pharm. Sci.* 110 (5), 2083–2092. https://doi.org/10.1016/j.xphs.2020.11.041.

Bawuah, P., Evans, M., Lura, A., Farell, D.J., Barrie, P.J., Kleinebudde, P., Markl, D., Zeitler, J.A., 2023. At-line porosity sensing for non-destructive disintegration testing in immediate release tablets. *J. Pharm. Sci. X.* 5, 100186. https://doi.org/10.1016/j.ijpx.2023.100186.

Besseling, R., Damen, M., Tran, T., Nguyen, T., van den Dries, K., Oostra, W., Gerich, A., 2015. An Efficient, Maintenance Free and Approved Method for Spectroscopic Control and Monitoring of Blend Uniformity: The Moving F-Test. *J. Pharm. Biomed. Anal.* 114, 471–481. https://doi.org/10.1016/j.jpba.2015.06.019.

Cameron, A., Briens, L., 2019a. An Investigation of Magnesium Stearate Performance in a V-Blender through Passive Vibration Measurements. *AAPS PharmSciTech.* 20, 199. https://doi.org/10.1208/s12249-019-1402-3.

Cameron, A., Briens, L., 2019b. Monitoring Magnesium Stearate Blending in a V-Blender through Passive Vibration Measurements. *AAPS PharmSciTech.* 20, 1–11. https://doi.org/10.1208/s12249-019-1469-x.

Crouter, A., Briens, L., 2016. Monitoring Lubricant Addition Using Passive Acoustic Emissions in a V-Blender. *Powd. Technol.* 301, 1119–1129. https://doi.org/10.1016/j.powtec.2016.07.051.

Dansereau, R., Peck, G.E., 1987. The Effect of the Variability in the Physical and Chemical Properties of Magnesium Stearate on the Properties of Compressed Tablets. *Drug Dev. Ind. Pharm.* 13 (6), 975–999. https://doi.org/10.3109/03639048709068365.

De Backere, C., De Beer, T., Vervaet, C., Vanhoorne, V., 2020. Evaluation of an External Lubrication System Implemented in a Compaction Simulator. *Int. J. Pharm.* 587, 119675. https://doi.org/10.1016/j.ijpharm.2020.119675.

De Backere, C., De Beer, T., Vervaet, C., Vanhoorne, V., 2023a. Upscaling of External Lubrication from a Compaction Simulator to a Rotary Tablet Press. *Int. J. Pharm.* 633, 122616. https://doi.org/10.1016/j.ijpharm.2023.122616.

De Backere, C., Surmont, M., De Beer, T., Vervaet, C., Vanhoorne, V., 2023b. Screening of Lubricants Towards Their Applicability for External Lubrication. *Int. J. Pharm.* 632, 122553. https://doi.org/10.1016/j.ijpharm.2022.122553.

Duong, N.-H., Arratia, P., Muzzio, F.J., Lange, A., Timmermans, J., Reynolds, S., 2003. A Homogeneity Study Using Nir Spectroscopy: Tracking Magnesium Stearate in Bohle Bin-Blender. *Drug Dev. Ind. Pharm.* 29 (6), 679–687. https://doi.org/10.1081/DDC-120021317.

Ebube, N.K., Thosar, S.S., Roberts, R.A., Kemper, M.S., Rubinovitz, R., Martin, D.L., Reier, G.E., Wheatley, T.A., Shukla, A.J., 1998. Application of near-Infrared Spectroscopy for Nondestructive Analysis of Avicel® Powders and Tablets. *Pharm. Dev. Technol.* 4 (1), 19–26. https://doi.org/10.1080/10837459908984220.

European Pharmacopoeia. 2024. "16 Monographs L-P; Magnesium Stearate." 11.5.

Fahiq, A.M.B., Mehrotra, A., Hammond, S.V., Muzzio, F.J., 2007. Effect of Moisture and Magnesium Stearate Concentration on Flow Properties of Cohesive Granular Materials. *Int. J. Pharm.* 336 (2), 338–345. https://doi.org/10.1016/j.ijpharm.2006.12.024.

FDA. 2004a. "Pharmaceutical cGMPS for the 21st Century—a Risk-Based Approach".

FDA. 2004b. "Guidance for Industry: PAT – A Framework for Innovative Pharmaceutical Development, Manufacturing and Quality Assurance.".

FDA. 2021. "Development and Submission of near Infrared Analytical Procedures - Guidance for Industry".

Fell, J.D., Newton, J.M., 1970. Determination of Tablet Strength by the Diametral-Compression Test. *J. Pharm. Sci.* 59 (5), 688–691. https://doi.org/10.1002/jps.2600590523.

Fonteyne, M., Vercruysse, J., De Leersnyder, F., Van Snick, B., Vervaet, C., Remon, J.P., De Beer, T., 2015. Process Analytical Technology for Continuous Manufacturing of Solid-Dosage Forms. *Trends. Anal. Chem.* 67, 159–166. https://doi.org/10.1016/j.trac.2015.01.011.

Hafeez Hussain, M.S., York, P., Timmins, P., 1988. A study of the formation of magnesium stearate film on sodium chloride using energy-dispersive X-ray analysis. *Int. J. Pharm.* 42 (1–3), 89–95. https://doi.org/10.1016/0378-5173(88)90164-0.

Herzberg, M., Rekis, T., Støttrup Larsen, A., Gonzalez, A., Rantanen, J., Østergaard Madsen, A., 2023. The structure of magnesium stearate trihydrate determined from a micrometre-sized single crystal using a microfocused synchrotron X-ray beam. *Acta Crystallogr. B Struct. Sci. Cryst. Eng. Mater.* 79 (4), 330–335. https://doi.org/10.1107/S2052520623005607.

Hinz, D.C., 2006. Process Analytical Technologies in the Pharmaceutical Industry: The FDA's PAT Initiative. *Anal Bioanal Chem.* 384, 1036–1042. https://doi.org/10.1007/s00216-005-3394-y.

ICH. 2009. "Guideline Q8 (R2) on Pharmaceutical Development." EMA/CHMP/ICH/167068/2004.

ICH. 2011. "Q8, Q9, and Q10 Questions and Answers(R4)." EMEA/CHMP/ICH/265145/2009.

ICH. 2023. "Guideline Q13 on Continuous Manufacturing of Drug Substances and Drug Products." EMA/CHMP/ICH/427817/2021.

ICH. 2024. "Q14 Analytical Procedure Development." EMA/CHMP/ICH/195040/2022.

Jarosz, P.J., Parrott, E.K., 1984. Effect of Lubricants on the Tensile Strengths of Tablets. *Drug Dev. Ind. Pharm.* 10 (2), 259–273. https://doi.org/10.3109/03639048409064649.

Kim, E.J., Kim, J.H., Kim, M.-S., Jeong, S.H., Choi, D.H., 2021. Process Analytical Technology Tools for Monitoring Pharmaceutical Unit Operations: A Control Strategy for Continuous Process Verification. *Pharmaceutics.* 13 (6), 919. https://doi.org/10.3390/pharmaceutics13060919.

Kushner IV, J., 2012. Incorporating Turbula mixers into a blending scale-up model for evaluating the effect of magnesium stearate on tablet tensile strength and bulk specific volume. Int. J. Pharm. 429 (1–2), 1–11. https://doi.org/10.1016/j.ijpharm.2012.02.040.

Kushner IV, J., Moore, F., 2010. Scale-up Model Describing the Impact of Lubrication on Tablet Tensile Strength. Int. J. Pharm. 399 (1–2), 19–30. https://doi.org/10.1016/j.ijpharm.2010.07.033.

Lee, S.u.L., O'Connor, T.F., Yang, X., Cruz, C.N., Chatterjee, S., Madurawe, R.D., Moore, C.M.V., Yu, L.X., Woodcock, J., 2015. Modernizing Pharmaceutical Manufacturing: From Batch to Continuous Production. *J. Pharm. Innov.* 10 (3), 191–199. https://doi.org/10.1007/s12247-015-9215-8.

Li, J., Wu, Y., 2014. Lubricants in Pharmaceutical Solid Dosage Forms. *Lubricants.* 2 (1), 21–43. https://doi.org/10.3390/lubricants2010021.

Markl, D., Sauerwein, J., Goodwin, D.J., van den Ban, S., Zeitler, J.A., 2017. Non-Destructive Determination of Disintegration Time and Dissolution in Immediate Release Tablets by Terahertz Transmission Measurements. *Pharm. Res.* 34 (5), 1012–1022. https://doi.org/10.1007/s11095-017-2108-4.

Markl, D., Warman, M., Dumarey, M., Bergman, E.L., Folestad, S., Shi, Z., Manley, L.F., Goodwin, D.J., Zeitler, J.A., 2020. Review of Real-Time Release Testing of Pharmaceutical Tablets: State-of-the Art, Challenges and Future Perspective. *Int. J. Pharm.* 582, 119353. https://doi.org/10.1016/j.ijpharm.2020.119353.

Marwaha, S.B., Rubinstein, M.H., 1987. Structure-lubricity evaluation of magnesium stearate. *Int. J. Pharm.* 43, 249–255. https://doi.org/10.1016/0378-5173(88)90281-5.

Mehrotra, A., Llusa, M., Faqih, A., Levin, M., Muzzio, F.J., 2007. Influence of Shear Intensity and Total Shear on Properties of Blends and Tablets of Lactose and

Cellulose Lubricated with Magnesium Stearate. *Int. J. Pharm.* 336 (2), 284–291. https://doi.org/10.1016/j.ijpharm.2006.12.013.
Nakagawa, H., Kano, M., Hasebe, S., Suzuki, T., Wakiyama, N., 2013. Real-Time Monitoring of Lubrication Properties of Magnesium Stearate Using Nir Spectrometer and Thermal Effusivity Sensor. *Int. J. Pharm.* 441 (1–2), 402–413. https://doi.org/10.1016/j.ijpharm.2012.11.014.
Otsuka, M., Yamane, I., 2006. Prediction of Tablet Hardness Based on near Infrared Spectra of Raw Mixed Powders by Chemometrics. *J. Pharm. Sci.* 95 (7), 1425–1433. https://doi.org/10.1002/jps.20514.
Otsuka, M., Yamane, I., 2009. Prediction of Tablet Properties Based on near Infrared Spectra of Raw Mixed Powders by Chemometrics: Scale-up Factor of Blending and Tableting Processes. *J. Pharm. Sci.* 98 (11), 4296–4305. https://doi.org/10.1002/jps.21748.
Paul, S., Sun, C.C., 2018. Systematic Evaluation of Common Lubricants for Optimal Use in Tablet Formulation. *Eur. J. Pharm. Sci.* 117, 118–127. https://doi.org/10.1016/j.ejps.2018.02.013.
Plumb, K., 2005. Continuous Processing in the Pharmaceutical Industry - Changing the Mindset. *Chem. Eng. Res. Des.* 83 (6), 730–778. https://doi.org/10.1205/cherd.04359.
Podczeck, F., Mia, Y., 1996. The Influence of Particle Size and Shape on the Angle of Internal Friction and the Flow Factor of Unlubricated and Lubricated Powders. *Int. J. Pharm.* 144 (2), 187–194. https://doi.org/10.1016/S0378-5173(96)04755-2.
Puckhaber, D., Finke, J.H., David, S., Serratoni, M., Zafar, U., John, E., Juhnke, M., Kwade, A., 2022. Prediction of the Impact of Lubrication on Tablet Compactibility. *Int. J. Pharm.* 617, 121557. https://doi.org/10.1016/j.ijpharm.2022.121557.
Puckhaber, D., Kwade, A., Finke, J.H., 2023. Investigation of Dispersion Kinetics of Particulate Lubricants and Their Effect on the Mechanical Strength of MCC Tablets. *Pharm. Res.* 40 (10), 2479–2492. https://doi.org/10.1007/s11095-023-03602-0.
Raymond, C.R., Sheskey, P.J., Owen, S.C., 2009. Handbook of Pharmaceutical Excipients. Pharmaceutical Press.
Ryshkewitch, E., 1953. Compression Strength of Porous Sintered Alumina and Zirconia. *J. Am. Ceram. Soc.* 36 (2), 65–68. https://doi.org/10.1111/j.1151-2916.1953.tb12837.x.
Shah, A.C., Mlodozeniec, A.R., 1977. Mechanism of Surface Lubrication: Influence of Duration of Lubricant-Excipient Mixing on Processing Characteristics of Powders and Properties of Compressed Tablets. *J. Pharm. Sci.* 66 (10), 1377–1382. https://doi.org/10.1002/jps.2600661006.
Shah, N.H., Stiel, D., Weiss, D., Infeld, M.H., Malick, A.W., 1986. Evaluation of Two New Tablet Lubricants -Sodium Stearyl Fumarate and Glyceryl Behenate. Measurement of Physical Parameters (Compaction, Ejection and Residual Forces) in the Tableting Process and the Effect on the Dissolution Rate. *Drug Dev. Ind. Pharm.* 12 (8–9), 1329–1346. https://doi.org/10.3109/03639048609065862.
Singh, R., Sahay, A., Karry, K.M., Muzzio, F., Ierapetritou, M., Ramachandran, R., 2014. Implementation of an Advanced Hybrid MPC–PID Control System Using Pat Tools into a Direct Compaction Continuous Pharmaceutical Tablet Manufacturing Pilot Plant. *Int. J. Pharm.* 473 (1), 38–54. https://doi.org/10.1016/j.ijpharm.2014.06.045.
Skelbæk-Pedersen, A.L., Anuschek, M., Kvistgaard Vilhelmsen, T., Rantanen, J., Zeitler, A., 2020. Non-destructive quantification of fragmentation within tablets after compression from scattering analysis of terahertz transmission measurements. *Int. J. Pharm.* 588 (1), 119769. https://doi.org/10.1016/j.ijpharm.2020.119769.
Stranzinger, S., Faulhammer, E., Li, J., Dong, R., Khinast, J.G., Zeitler, J.A., Markl, D., 2019. Measuring Bulk Density Variations in a Moving Powder Bed Via Terahertz in-Line Sensing. *Powder Technol.* 344, 152–160. https://doi.org/10.1016/j.powtec.2018.11.106.
Strickland Jr., W.A., Nelson, E., Busse, L.W., Higuchi, T., 1956. The Physics of Tablet Compression Ix. Fundamental Aspects of Tablet Lubrication. *J. Am. Pharm. Assoc.* 45 (1), 51–55. https://doi.org/10.1002/jps.3030450116.
Su, Q., Ganesh, S., Moreno, M., Bommireddy, Y., Gonzalez, M., Reklaitis, G.V., Nagy, Z. K., 2019. A Perspective on Quality-by-Control (Qbc) in Pharmaceutical Continuous Manufacturing. *Comput. Chem. Eng.* 125, 216–231. https://doi.org/10.1016/j.compchemeng.2019.03.001.
Sun, C.C., 2015. Dependence of Ejection Force on Tableting Speed—a Compaction Simulation Study. *Powder. Technol.* 279, 123–126. https://doi.org/10.1016/j.powtec.2015.04.004.
Uchiyama, J., Kato, Y., Uemoto, Y., 2014. Evaluation of Risk and Benefit in Thermal Effusivity Sensor for Monitoring Lubrication Process in Pharmaceutical Product Manufacturing. *Drug Dev. Ind. Pharm.* 40 (8), 999–1005. https://doi.org/10.3109/03639045.2013.795581.
United States Pharmacopeia, 2024. General Chapter, <1062> Tablet Compression Characterization. USPNF. https://doi.org/10.31003/USPNF_M99395_02_01.
Uzunović, A., Vranić, E., 2007. Effect of Magnesium Stearate Concentration on Dissolution Properties of Ranitidine Hydrochloride Coated Tablets. *Bosn. J. Basic Med.* 7 (3), 279–283. https://doi.org/10.17305/bjbms.2007.3060.
Wang, J., Wen, H., Desai, D., 2010. Lubrication in Tablet Formulations. *Eur. J. Pharm. Biopharm.* 75 (1), 1–15. https://doi.org/10.1016/j.ejpb.2010.01.007.
Wada, Y., Matsubara, T., 1994. Pseudopolymorphism and lubricating properties of magnesium stearate. *Powder Technol.* 78 (2), 109–114. https://doi.org/10.1016/0032-5910(93)02782-6.
Yoshihashi, Y., Sato, M., Kawano, Y., Yonemochi, E., Terada, K., 2013. Evaluation of Physicochemical Properties on the Blending Process of Pharmaceutical Granules with Magnesium Stearate by Thermal Effusivity Sensor. *J. Therm. Anal. Calorim.* 113, 1281–1285. https://doi.org/10.1007/s10973-013-3018-2.
Yu, L.X., 2008. Pharmaceutical Quality by Design: Product and Process Development. Understanding and Control. Pharm. Res. 25, 781–791. https://doi.org/10.1007/s11095-007-9511-1.
Zeitler, J.A., Taday, P.F., Newnham, D.A., Pepper, M., Gordon, K.C., Rades, T., 2010. Terahertz Pulsed Spectroscopy and Imaging in the Pharmaceutical Setting-a Review. *J. Pharm. Pharmacol.* 59 (2), 209–223. https://doi.org/10.1211/jpp.59.2.0008.
Zuurman, K., Van der Voort Maarschalk, K., Bolhuis, G.K., 1999. Effect of magnesium stearate on bonding and porosity expansion of tablets produced from materials with different consolidation properties. *Int. J. Pharm.* 179 (1), 107–155. https://doi.org/10.1016/S0378-5173(98)00389-5.